IEEE Access
Multidisciplinary | Rapid Review | Open Access Journal

Received May 22, 2022, accepted June 6, 2022, date of publication June 13, 2022, date of current version June 17, 2022.

Digital Object Identifier 10.1109/ACCESS.2022.3182241

Research on Multistrategy Improved Evolutionary Sparrow Search Algorithm and Its Application

BINGWEI GAO, WEI SHEN, HAO GUAN, LINTAO ZHENG, AND WEI ZHANG

School of Mechanical and Power Engineering, Harbin University of Science and Technology, Harbin 150080, China
Key Laboratory of Advanced Manufacturing and Intelligent Technology, Ministry of Education, Harbin University of Science and Technology, Harbin 150080, China

Corresponding author: Bingwei Gao (gaobingwei_happy@163.com)

This work was supported in part by the Natural Science Foundation of Heilongjiang Province of China under Grant LH2019E064, and in part by the National Natural Science Foundation of China under Grant 52075134.

ABSTRACT To address the problem of the sparrow search algorithm (SSA) has poor global search ability, weak local development ability, and easily falls into the local optimal solution, a multi-strategy improved evolutionary sparrow search algorithm (MSSA) is proposed. The introduction of the tent chaotic map improves the diversity of the initialization population, accelerates algorithm convergence, and improves convergence accuracy. Endow sparrow finders with a random search ability to coordinate the balance between global search and local development. To discover dangerous sparrow individuals, the mutation evolution operation is completed, and a greedy strategy is combined to improve the processing ability of the algorithm for local optimal solutions and make full use of each sparrow individual. Six benchmark functions were used to comprehensively verify the feasibility of the proposed algorithm based on four aspects: optimization ability, robustness, convergence ability, and optimization trajectory. These results indicate that the proposed algorithm is superior. Finally, through the comparison and analysis of the parameter identification and control strategies of the two servo systems in practical application, on the one hand, the advantages of the proposed algorithm in practical engineering applications are illustrated. In addition, a fuzzy PID control strategy based on MSSA is proposed. By adding step, sinusoidal, triangular wave and disturbance signals, simulation experiments show that the control strategy can significantly improve the dynamic and steady performance of the servo system.

INDEX TERMS Sparrow search algorithm, multi-strategy, identification, fuzzy PID.

I. INTRODUCTION

In most practical problems and engineering applications, researchers are inspired by biological and natural physical phenomena and propose metaheuristic algorithms with simplicity, flexibility, and high robustness [1]. Common meta-heuristic algorithms include the particle swarm optimization (PSO) [2], glowworm swarm optimization (GSO) [3], genetic algorithm (GA) [4], whale optimization algorithm (WOA) [5], war strategy optimization algorithm (WSOA) [6], and artificial chemical reaction optimization algorithm (ACROA) [7]. Because they are easy to implement and can effectively deal with global and large-scale optimization problems, they are widely used in multi-objective optimization, parameter identification, parameter optimization, and many other fields. The sparrow search algorithm (SSA) is a heuristic swarm intelligence optimization algorithm proposed by Xue and Shen [8] in 2020, based on the biological behavior of sparrow foraging and predator avoidance. SSA has a unique search model and excellent optimization ability, but it has defects, such as being easy to fall into a local optimum.

Considering the limitations of practical applications and the commonality of the advantages and disadvantages of each meta-heuristic algorithm, many scholars have proposed numerous novel and improved meta-heuristic algorithms to meet engineering needs. Ab Aziz *et al.* [9] proposed an adaptive gravity search algorithm that switches between synchronous and asynchronous updates to provide diversity to the population and to avoid premature convergence. In [10], all algorithms and applications of plant intelligence were first collected and searched. Information is provided about plant intelligence algorithms, such as the flower pollination algorithm, invasive weed optimization, paddy field algorithm,

The associate editor coordinating the review of this manuscript and approving it for publication was Engang Tian.

root mass optimization algorithm, artificial plant optimization algorithm, sapling growing up algorithm, photosynthetic algorithm, plant growth optimization, root growth algorithm, strawberry algorithm as plant propagation algorithm, runner root algorithm, path planning algorithm, and rooted tree optimization. Deng *et al.* [11] proposed a particle swarm optimization algorithm for square-wave-triggered exploration and development, using a square-wave trigger mechanism to optimize the update method and improve the convergence speed and accuracy of the algorithm. Liu *et al.* [12] proposed a hybrid optimization algorithm for grey wolves and coyotes, using a dynamic adjustment scheme combined with a sinusoidal crossover strategy to improve the search efficiency and convergence speed of the algorithm. Zhang *et al.* [13] proposed a multi-strategy golden sine chimpanzee optimization algorithm, which introduced the Halton sequence, convergence factor, and weight factor, and combined them with the golden sine correlation idea to improve the algorithm's ability to handle local optimal values. Yu *et al.* [14] proposed a gray wolf localization algorithm based on the beetle search algorithm, which transformed the node localization problem into function-constrained optimization to prevent the grey wolf algorithm from falling into local optimization in later iterations. In [15], different ergodic chaotic systems were used for the first time to generate chaotic values instead of random values in optics inspired optimization (OIO) processes to enhance the global convergence speed and prevent stuck in local solutions of the classical OIO algorithm. Furthermore, a new application area for chaos was proposed.

New and improved metaheuristic algorithms have also been applied in various fields [16]. Liu *et al.* [17] designed an immune cooperative particle swarm algorithm for the multiparameter identification of permanent magnet synchronous motors. This method can effectively identify the changing values of parameters such as the motor resistance and rotor flux linkage. In [18], studies of two recently proposed algorithms, namely ray optimization and optics inspired optimization, were compiled, and the performance analysis of light-based intelligent optimization algorithms on unconstrained benchmark functions and constrained real engineering design problems was performed under equal conditions for the first time. The results obtained show that ray optimization is superior and effectively solves many complex problems. Mohammed and Rashid [19] used the hunting mechanism of the grey wolf optimization algorithm to embed the whale swarm optimization algorithm development stage and applied the improved algorithm to solve the pressure vessel design engineering problem, which improved the quality of the solution and avoided local optima. Yu *et al.* [20] used the H∞ theory to reduce the search space and integrated information entropy to improve the particle swarm optimization algorithm and optimize the parameters of the motion controller of the mobile robot. The experimental results showed that the negative pressure adsorption motor of the grid pipeline robot had a good control effect along with circular motion during the adsorption process. Wei *et al.* [21] used a fusion-improved ant colony algorithm and a DWA algorithm to plan the road strength of mobile robots, which improved their robot's ability and speed to avoid obstacles. In [22], optics inspired optimization (OIO) for the first time was designed as a solution search strategy for traveling tournament problem which is one of the current sport's problems and aids in minimizing transportation and total movement of teams.

In summary, the improvements and applications of metaheuristic algorithms have emerged in an endless stream, each with its advantages. Considering the novelty and limitations of the sparrow search algorithm, strategies suitable for solving practical engineering problems are explored. This research proposes a multi-strategy improved evolutionary sparrow search algorithm (MSSA). The main contributions of this research are as follows.

- We propose an improved SSA. MSSA provides three major improvements over the base SSA:
  1. MSSA uses a tent chaotic map to initialize the sparrow population, distributes the sparrow individuals evenly, and ensures the diversity of the initial population of the algorithm.
  2. Endow sparrow searchers with random searchability, accelerate algorithm convergence, and improve algorithm searchability.
  3. To discover dangerous sparrow individuals, perform evolutionary mutation operations and combine the greedy strategy to establish the optimal value of the sparrow population, making full use of all individuals in the sparrow population.
- Six classical test functions were used in the simulation experiment to verify the superiority of the MSSA algorithm from four aspects: optimization ability, robustness, convergence ability, and optimization trajectory.
- A comparison of the practical application designs of the two servo systems shows that MSSA has advantages over the other algorithms. A fuzzy PID control strategy based on the MSSA is proposed, which improves the control performance and precision of the servo system.

The remainder of this paper is organized as follows. Section II provides a brief overview of the standard SSA. Section III describes the proposed MSSA in detail, including the tent chaos map, lévy-flight strategy, and evolution strategy. Section IV demonstrates the superiority of the MSSA and illustrates the advantages of the method through simulations and comparisons. Section V simulates the application research of the servo system, demonstrates the superiority of the MSSA, proposes a fuzzy PID control strategy based on the MSSA, and analyzes the experimental results. Finally, Section VI presents the conclusions of this research, including directions for future improvement.

II. THE STANDARD SPARROW SEARCH ALGORITHM

The sparrow search algorithm realizes the optimal search for model parameters by simulating the behavior of sparrow

foraging and predator avoidance [23]. Assuming that the population of the standard SSA is N, the optimal solution is searched in the D-dimensional region.

The finder location is updated as follows:

$$x_{id}^{t+1} = \begin{cases} x_{id}^{t} \cdot exp\left(\frac{-i}{\alpha \cdot T}\right), & R_2 < ST \\ x_{id}^{t} + Q \cdot L, & R_2 \geq ST \end{cases} \quad (1)$$

where x_{id}^{t} is the position of the sparrow, T is the number of iterations, α is a uniform random number between (0,1], Q is a random number that conforms to a normal distribution, L is a unit vector, R_2 is the warning value, ST is the safety value.

The joiner location is updated as follows:

$$x_{id}^{t+1} = \begin{cases} Q \cdot \exp\left(\frac{x\omega_d^t - x_{id}^t}{i^2}\right), & i > \frac{n}{2} \\ xb_d^{t+1} + \left|x_{id}^t - xb_d^{t+1}\right| A^+ \cdot L, & otherwise \end{cases} \quad (2)$$

where $x\omega_d^t$ represents the worst position, xb_d^{t+1} represents the individual position with the best fitness in the (t+1) iteration, A represents the matrix, $A^+ = A^T(AA^T)^{-1}$.

The vigilante location has been updated to:

$$x_{id}^{t+1} = \begin{cases} xb_d^t + \beta\left(x_{id}^t - xb_d^t\right), & f_i \neq f_g \\ x_{id}^t + K\left(\frac{x_{id}^t - xw_d^t}{|f_i - f_\omega| + \varepsilon}\right), & f_i = f_g \end{cases} \quad (3)$$

where β is the step size control parameter, K is a uniform random number between [-1,1], f_i is the fitness of the current sparrow, f_g is the best fitness, f_ω is the worst fitness, ε is a sufficiently small number to avoid the case where the denominator is 0.

III. THE MULTI-STRATEGY IMPROVED EVOLUTIONARY SPARROW SEARCH ALGORITHM

A. TENT CHAOS MAP STRATEGY

The initial position of the individual population is very important for optimizing the performance of the meta-heuristic algorithm [24]-[26]. The traversal of the tent chaotic map is uniform and random, which allows the algorithm to easily jump out of the local optimal solution and simultaneously improves the global search ability, thereby maintaining the diversity of the population [27]-[29]. Therefore, the tent chaotic map is introduced to initialize the sparrow population such that the population is evenly distributed, and the convergence speed and optimization accuracy of the algorithm is improved. The formula used is as follows.

$$x_{k+1} = \begin{cases} \frac{x_k}{\theta} - r/N, & x_k \in [0, \theta) \\ \frac{1-x_k}{(1-\theta)} - r/N, & x_k \in [\theta, 1] \end{cases} \quad (4)$$

where N is the population size, θ is the chaos factor, r and θ are uniform random numbers between (0,1), k is the number of iterations, and $x_k \in (0, 1)$. When $r = 0$, with the change of θ, the generated sequence is as shown in Figure 1(a), and the distribution histogram is as shown in Figure 1(b).

It can be observed from Figure 1(a) that the tent chaotic map has a uniform distribution function and good correlation.

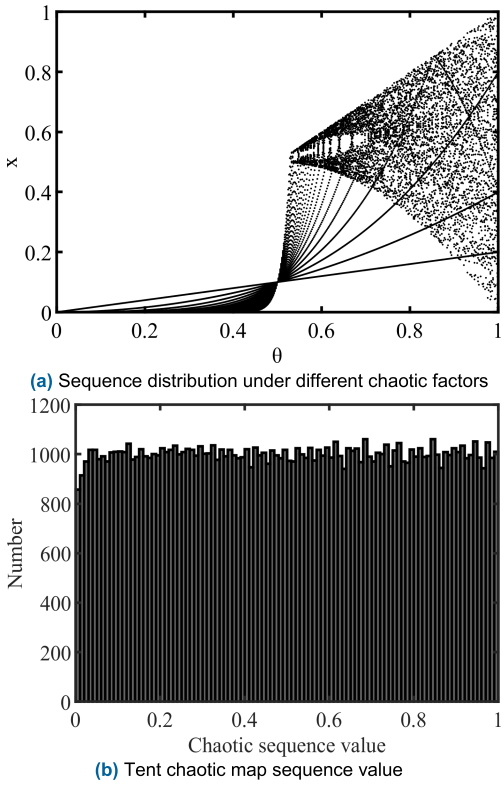

(a) Sequence distribution under different chaotic factors

(b) Tent chaotic map sequence value

FIGURE 1. Tent chaotic map sequence.

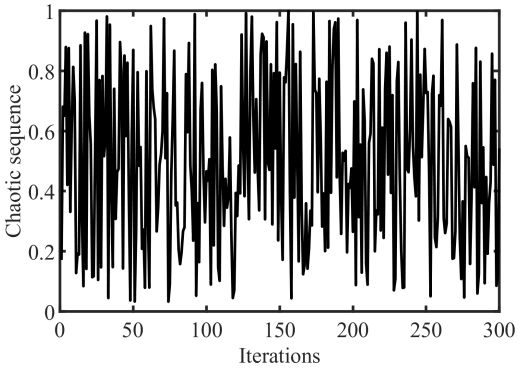

FIGURE 2. Tent chaotic map values.

With an increase in the value of θ, the variation range of the x value expanded, and the performance became more abundant. In particular, $\theta = 0.5$, the system exhibits a short-period state, and when θ approaches 1, the population randomness is optimal. As shown in Figure 1(b), the distribution histogram counts 100,000 values as samples, with an interval of 0.01. At this time, the ideal sequence means should be 1000. It can be observed that the mean of the tent mapping sequence satisfied the requirements. Therefore, the selected tent map with $\theta = 0.9$ initializes the population, and the number of iterations is set to 300. The tent chaotic map values are shown in Figure 2.

Eq. (5) is used to map the variable value generated by the tent chaotic map to sparrow individual to realize the sparrow

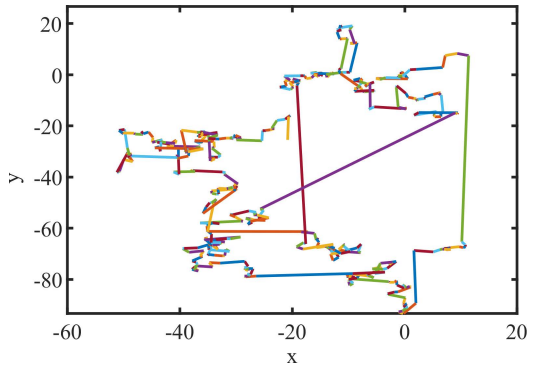

FIGURE 3. Schematic diagram of lévy-Flight.

population initialization.

$$X = X_{LB} + (X_{UB} - X_{LB})X_{K+1} \tag{5}$$

where X is the individual after mapping, X_{UB} and X_{LB} are the upper and lower limits of each individual and each dimension, respectively.

B. LÉVY-FLIGHT STRATEGY

In the optimization process of traditional SSA, there are defects, such as weak global search ability, weak local development, and ease of falling into the local optimum, resulting in insufficient search accuracy of the algorithm [30].

Levy flight is a random search algorithm that obeys the levy distribution and is a method of walking that alternates short-distance searches and occasional longer-distance walks. Figure 3 shows a schematic of the Levy flight with the simulation step size set to 500. Levy flight makes the change in individual position more flexible and has a larger search range, so it can prevent the algorithm from falling into a stagnant state, thus promoting the discoverer to have good global searchability.

The finder location update that introduces levy-flight is as follows:

$$x_{id}^{t+1} = \begin{cases} x_{id}^{t} \cdot exp\left(\frac{-i}{\alpha \cdot T}\right) \cdot levy, & R_2 < ST \\ x_{id}^{t} \cdot levy + Q \cdot L, & R_2 \geq ST \end{cases} \tag{6}$$

where *levy* satisfies the lévy distribution, and its mathematical expression is as follows:

$$levy = \gamma \frac{\mu}{|v|^{\frac{1}{\vartheta}}}(f_g - x_{id}^{t}) \tag{7}$$

where γ is the flight scale of the levy-flight, ϑ is the levy-flight factor, which is a random number of (1,3], $\tau(\cdot)$ is the gamma function, $\mu \sim N(0, \sigma_\mu^2)$, $v \sim N(0, \sigma_v^2)$, $\sigma_v = 1$, $\sigma_\mu = \left\{\frac{\tau(1+\vartheta)\cdot\sin(\frac{\pi\vartheta}{2})}{\tau(\frac{1+\vartheta}{2})\cdot\vartheta\cdot\frac{\vartheta-1}{2}}\right\}^{\frac{1}{\vartheta}}$.

C. EVOLUTION STRATEGY

When the sparrow is at the edge of the population, its search method jumps to the optimal solution with relatively small step size, and it has the disadvantage that it is difficult to eliminate the local extremum constraint. As shown in Figure 4,

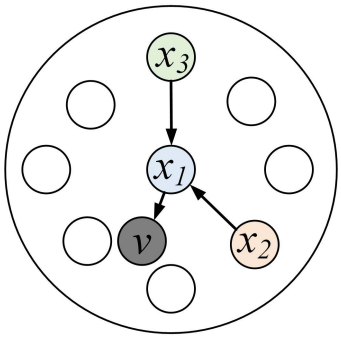

FIGURE 4. Schematic diagram of differential mutation strategy.

differential evolution refers to the cooperation and competition among individuals in the group to guide the direction of the optimization search. The mathematical description is given by the following equation. The optimal point corresponding to an individual in the population was assumed to be an elite individual. When the algorithm stops updating, two suboptimal solutions are selected and the current optimal solution is mutated through a crossover operation.

$$v = x_1 + F \cdot (x_2 - x_3) \tag{8}$$

where x_1, x_2, x_3 are three different individuals randomly selected from each other in the current population, F is the variation factor, and v is the variation individual corresponding to the target individual.

When the individual sparrows are threatened at the edge of the population, to avoid the phenomenon of 'jumping', the current optimal position and the optimal position of the first iteration are selected to perform the crossover operation. Although the ability of the algorithm to escape the local space is improved through the above mutation strategy, it is impossible to determine whether the new position obtained after perturbation mutation is better than the original position. Thus, the greedy selection strategy is used. According to the value of the fitness function, a better position is selected from the target individual xb_d^{t+1} and mutant individual and the better individual is retained in the next generation. If the mutant individual is better than the target individual, the search direction can be changed so that the algorithm can jump out of the current local optimal area. After introducing the evolution strategy, the position update formula for vigilante is as follows:

$$x_{id}^{t+1} = \begin{cases} xb_d^{t} + \omega\left(x_{id}^{t} - xb_d^{t}\right), & f_i \neq f_g \\ x_{id}^{t} + K\left(\frac{x_{id}^{t} - xw_d^{t}}{|f_i - f_\omega| + \varepsilon}\right), & f_i = f_g \end{cases} \tag{9}$$

$$\omega = \begin{cases} \omega_{min} + \\ (\omega_{max} - \omega_{min})\left(xb_d^{1} - xb_d^{t} + \varepsilon\right)\frac{(x_{id}^{t} - xb_d^{1})}{(x_{id}^{t} - xb_d^{t})} \end{cases} \tag{10}$$

where xb_d^1 is the individual position with the best fitness in the first iteration, ω_{min} is the minimum weight, ω_{max} is the maximum weight, f_{mb} is the fitness value of the target individual, and f_{by} is the fitness value of the mutant individual.

Algorithm 1 MSSA.

Input: Set the maximum number of iterations t_{max}. Define the evaluation function f. Randomly set N positions of sparrows $x_i^t (i = 1, 2, \ldots, N)$. Set $t = 0$.
Set the c value according to the optimization purpose. Initialize a population of N sparrows and define the relevant parameters.
G: the maximum iterations
PD: the number of the producers
SD: the number of the sparrows who perceive the danger
R2: the alarm value
Output: f_{best}: the best fitness value
x_{best}: the global optimal individual
1: **while** ($t < T_{max}$)
2: **For** i = 1: PD
3: Update the finder position using Eq. (6);
4: **For** i = 1: (PD+1): n
5: Update the follower position using Eq. (2);
6: **For** i = 1: SD
7: Update the watcher position using Eq. (9);
8: **End for**
9: Get the current new location;
10: If the new location is better than before, update it;
11: t = t + 1
12: **End while**
13: Return f_{best}, x_{best}.

D. MSSA IMPLEMENTATION PROCESS AND PSEUDO CODE

About the detailed information on the procedure of MSSA The specific implementation steps and pseudocode of the MSSA algorithm are as follows:

Step 1. Set the maximum number of iterations and define all algorithm parameters, including the number of discoverers m, number of early warnings s, dimension D, upper and lower limits of individual values lb, ub, learning rate ε, and number of iterations tmax, etc.

Step 2. The chaotic map randomly initializes the sparrow population position.

Step 3. Calculate the individual fitness of each sparrow, taking the first m individuals with higher fitness ability as discoverers, and the remaining (pop-m) individuals as followers, randomly selecting s individuals as early warnings.

Step 4. The finder conducts a random location flight search.

Step 5. Update the individual position of the follower.

Step 6. Randomly select alerters from the sparrow populations to determine whether they are threatened. The position is updated if the individual is not threatened and does not exceed the set maximum number of stagnant steps. If the individual is threatened, the mutation operation is performed, and the better fitness value position is selected by the greedy rule.

TABLE 1. Benchmark function information.

Function code	Function name	Value range	The optimal value
f_1	Sphere	[-100，100]	0
f_2	Rosenbrock	[-5.12，5.12]	0
f_3	Ackley	[-5.12，5.12]	0
f_4	Griewank	[-600，600]	0

Step 7. The individual position of the current population is recorded, and the sparrow individual with the best fitness value is selected.

Step 8. Update the number of iterations t = t + 1 and return to step 2. Repeat this step until t = tmax or the algorithm converges.

E. MSSA TIME COMPLEXITY

The time complexity of the basic SSA algorithm is O (N×D×tmax), where tmax is the maximum number of iterations. The time complexity analysis of the MSSA algorithm is as follows:

(1) The time complexity of introducing the Tent chaotic sequence to initialize the population is O (N×D), then the time complexity of MSSA is O (N×D×tmax+N×D) = O (N×D×tmax).

(2) Assuming that the time complexity of Levy flight is O (N×PD), the time complexity of the MSSA algorithm is O (N×D×tmax+N×PD) = O (N×D×tmax).

(3) The time complexity required to introduce the evolution strategy is O (N×SD), then the time complexity of the MSSA algorithm is O (N×D×tmax+N×SD) = O(N×D×tmax).

To sum up, the time complexity of the MSSA algorithm is O(N×D×tmax). It is observed that the MSSA algorithm proposed in this research has the same time complexity as the SSA algorithm.

IV. PERFORMANCE TESTING OF METAHEURISTIC ALGORITHMS

To further prove the optimization effect and algorithm performance of MSSA, four groups of benchmark functions are selected for simulation experiments. The specific function information is shown in Table 1. The experimental environment uses an Inter (R) Croe (TM) i7-10845hCPU, a PC with a main frequency of 2.3GHz and a memory of 16G, the operating system uses a 64-bit Windows11 system, and the programming language uses MATLAB R2020a. Using SSA, PSO, adaptive step-size PSO (APSO) [31], GSO, and improved adaptive step-size GSO (IASGSO) [32], these five algorithms are compared and analyzed.

The five comparison algorithms and MSSA were tested on four groups of test functions. To ensure the absolute fairness of the experimental environment and avoid randomness, all algorithms were set to the same common parameters: the population of each algorithm was 100.

The basic settings of the 6 algorithms are as follows:

(1) PSO and APSO: the cognitive learning factor is 2, the social learning factor is 2, the maximum particle movement

TABLE 2. Experimental results of MSSA and other 5 comparison algorithms on 4 groups of test functions.

Function code	Evaluation indicators	Algorithm error					
		PSO	APSO	GSO	IASGSO	SSA	MSSA
Low dimensional (D=30)							
f_1	Mean	8.82E-12	3.87E-20	2.53E-04	4.04E-08	3.19E-107	**6.87E-257**
	Standard deviation	1.10E-11	5.78E-20	2.41E-04	1.30E-08	6.32E-107	**1.36E-256**
f_2	Mean	8.31E-09	4.77E-17	9.63E-05	1.31E-20	2.82E-08	**6.75E-74**
	Standard deviation	9.14E-09	7.79E-17	1.00E-04	2.07E-20	4.08E-08	**1.34E-73**
f_3	Mean	1.88E-02	1.53E-05	1.45E-05	2.91E-10	8.88E-16	**3.77E-71**
	Standard deviation	8.33E-03	1.09E-05	1.07E-05	2.58E-10	7.89E-31	**7.46E-71**
f_4	Mean	1.16E-03	2.10E-04	1.63E-04	2.15E-07	**0.00E+00**	**0.00E+00**
	Standard deviation	1.94E-03	4.00E-04	2.97E-04	2.41E-07	**0.00E+00**	**0.00E+00**
High-dimensional (D=100)							
f_1	Mean	1.54E-33	5.37E-88	4.76E-10	7.63E-19	**0.00E+00**	**0.00E+00**
	Standard deviation	2.21E-33	1.03E-87	8.99E-10	1.24E-18	**0.00E+00**	**0.00E+00**
f_2	Mean	1.10E-30	**0.00E+00**	2.52E-12	1.34E-30	1.11E-13	**0.00E+00**
	Standard deviation	1.93E-30	**0.00E+00**	3.52E-12	2.24E-30	2.02E-13	**0.00E+00**
f_3	Mean	1.35E-15	8.88E-16	3.45E-08	8.88E-16	8.88E-16	**0.00E+00**
	Standard deviation	8.04E-16	7.89E-31	3.59E-08	9.86E-32	9.86E-32	**0.00E+00**
f_4	Mean	1.70E-03	7.40E-05	7.76E-12	**0.00E+00**	**0.00E+00**	**0.00E+00**
	Standard deviation	2.62E-03	1.46E-04	1.35E-11	**0.00E+00**	**0.00E+00**	**0.00E+00**

speed is 1, and the particle minimum movement speed is -1. The inertia weight of PSO is 0.7249, the maximum value of the APSO inertia factor is 0.95, and the minimum value is 0.4.

(2) GSO and IASGSO: The fluorescein volatility factor is 0.4, the fitness extraction ratio is 0.6, the domain change rate is 0.08, the domain threshold is 5, the perception radius is 5.12, and the decision radius is 5.12. The GSO step size is 0.1, the IASGSO maximum step size is 0.9, and the minimum step size is 0.1.

(3) SSA and MSSA: 20% of the population of finders, and 20% of sparrows are aware of the danger, and a safety threshold of 0.8. The MSSA Levi flight scale is 1, the Levi flight factor is 1.5, the minimum weight is 0.1, and the maximum weight is 0.9.

A. OPTIMIZE PERFORMANCE

f_1 and f_2 are multi-dimensional unimodal functions. These functions are difficult to solve and are suitable for testing the solving and optimization abilities of the algorithm. f_3 and f_4 are multidimensional and multimodal functions, which have multiple local optimal points and obstacles and are suitable for testing the ability of the algorithm to jump out of local optimal values. Table 2 lists the means and standard deviations of the six algorithms after running 100 times independently on different test functions under the 30 and 100 dimensions of the benchmark test function. The maximum number of iterations of all algorithms is 100 in the low-dimensional state and 500 in the high-dimensional state. The smaller the average value, the better the optimization performance of the algorithm, and the standard deviation indicates the stability of the system.

It can be seen from Table 2 that for the single-peak and multi-peak benchmark test functions, the MSSA is superior to the other five algorithms in terms of search accuracy and optimization stability, regardless of the dimensions. The MSSA converges to the theoretical optimum for the benchmark function f_4. Compared with classical optimization algorithms and their improved algorithms, the MSSA has great advantages in solution accuracy and robustness, and most of them can achieve the convergence accuracy given by the function. For example, for low-dimensional f_1, the mean and standard deviation of the MSSA is approximately 20 times that of the PSO, 12 times that of the APSO, 60 times that of the GSO, and 30 times that of the IASGSO, and 2 times that of the SSA. Under high-dimensional conditions, the MSSA can achieve the optimal value.

In summary, the MSSA is an optimization algorithm with good search accuracy and stability. However, whether it is a low-dimensional or high-dimensional benchmark function, the overall trend of the experimental results is similar, and the following analysis only selects the low-dimensional state for comparative robustness and convergence speed analysis.

B. ROBUSTNESS

Figure 5 shows a boxplot of the results obtained by the six algorithms independently solving the four benchmark functions in a low-dimensional state. By evaluating the maximum, minimum, median, and upper quartiles in the boxplot, outliers in the data can be visually identified [33], and the discrete distribution of the data can be determined to understand the state of the data distribution.

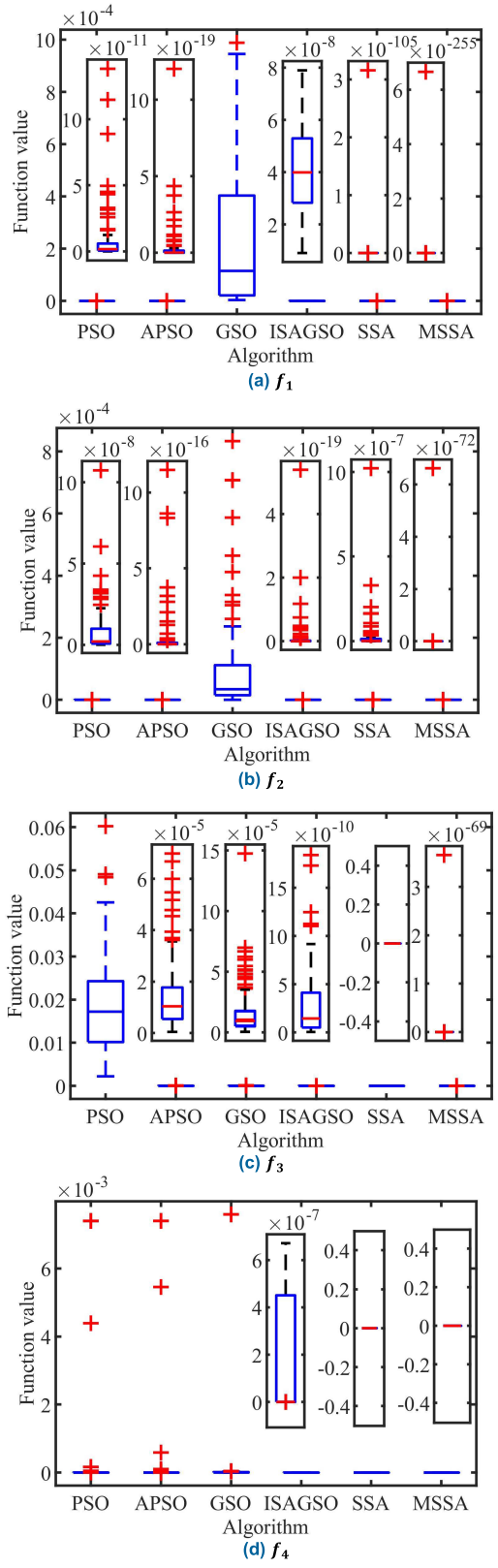

FIGURE 5. Convergence box plot of 6 algorithms.

It can be seen from Figure 5 that when solving, the outliers obtained by MSSA are fewer than those obtained by the comparison algorithm. When solving all test functions, except for the f_3 benchmark test function, the maximum, minimum, median, and upper quartiles of the MSSA algorithm in the boxplot were lower than those of other algorithms. This shows that the MSSA algorithm has a strong balance ability when dealing with different functions, and the distribution of convergence values is more centralized than the other comparison algorithms, which is better than other comparison algorithms, indicating that the MSSA algorithm has strong robustness. For f_3, combined with Table 2, it is observed that in the low-dimensional state, the MSSA optimization accuracy is higher than that of the other algorithms. Considering that the data of the boxplot SSA algorithm are more stable, it shows that the SSA has a local optimal value phenomenon for the benchmark function. The improvement in MSSA optimization accuracy shows that the improved algorithm can jump out of the local optimal value. This situation is more evident in a high-dimensional state. The SSA cannot eliminate the local optimal solution after 500 iterations, whereas the MSSA can find the optimal value.

C. CONVERGENCE PERFORMANCE

To demonstrate show the optimization speed and accuracy advantages of the MSSA algorithm. In the low-dimensional state, the convergence curves of the MSSA algorithm and the other five comparison algorithms on the four benchmark functions were drawn, and the maximum number of iterations of the algorithm was 100. The convergence curve is shown in Figure 6, and the ordinate in the figure is the optimal fitness value.

As shown in Figure 6, compared with PSO, APSO, GSO, IASGSO, and SSA, the MSSA algorithm has the fastest solution speed and absolute advantage. It finds the optimal solution position faster than other algorithms on all test functions and has obtained a good fitness value in the initial stage. It can be concluded that MSSA is competitive compared with the other five algorithms. For example, for the benchmark function f_4, the GSO, PSO, and APSO algorithms achieved good fitness values after approximately 50 iterations. The IASGSO and SSA were achieved after approximately the third iteration. The MSSA algorithm can achieve better convergence from the beginning.

D. MOVEMENT TRACK

After analyzing the test results of multiple groups of functions, fixed-dimension benchmark test functions that are difficult to solve are selected. Functional information is presented in Table 3. We tested the performance of the MSSA on the optimization of test samples and obtained the iterative trajectory of its population. The optimization performance of the MSSA algorithm can be observed more intuitively through 2D and 3D mathematical model diagrams and compared with the standard SSA algorithm. Figure 7 and Figure 8 show the 2-dimensional and 3-dimensional motion trajectories of the sparrow population movement on each benchmark function, respectively.

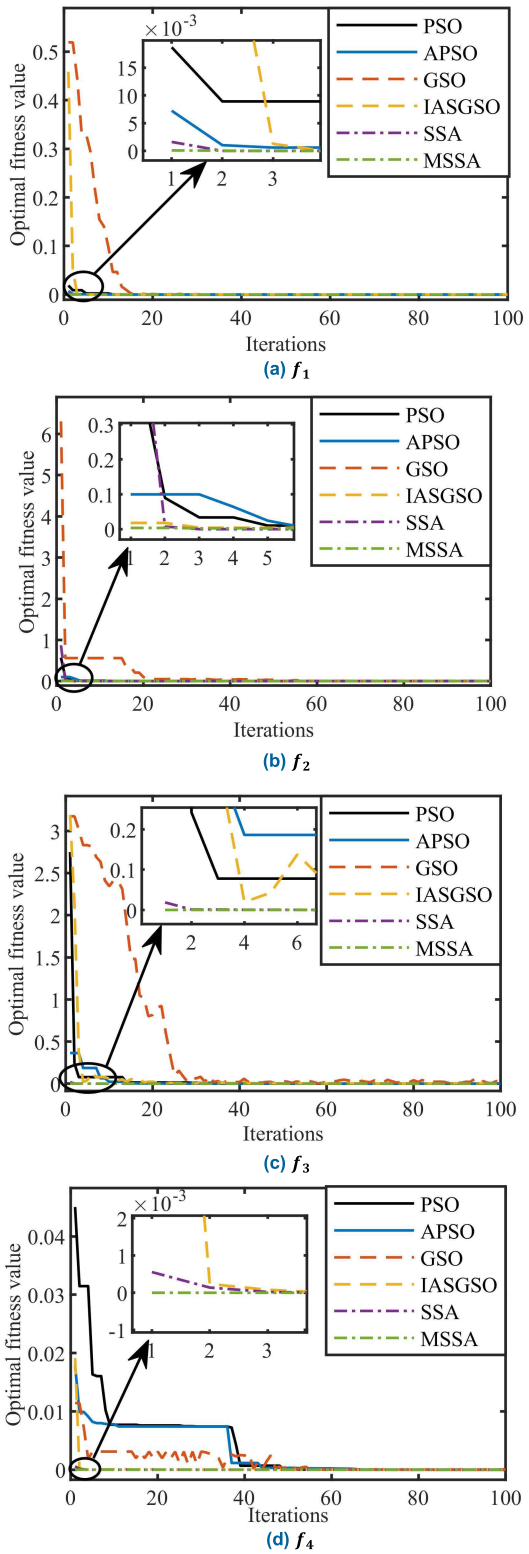

FIGURE 6. Convergence curves of 6 algorithms on 4 test functions.

It is observed that by using the fixed dimension test function, the individuals of the MSSA algorithm can all gather at the global optimal value or its vicinity, and fewer discrete points indicate that its optimization ability is strong. It can be

TABLE 3. Benchmark function information.

Function code	Function name	Value range	Dimension	The optimal value
f_5	Rastrigin	[-5.12, 5.12]	2	0
f_6	Matyas	[-5.12, 5.12]	2	0

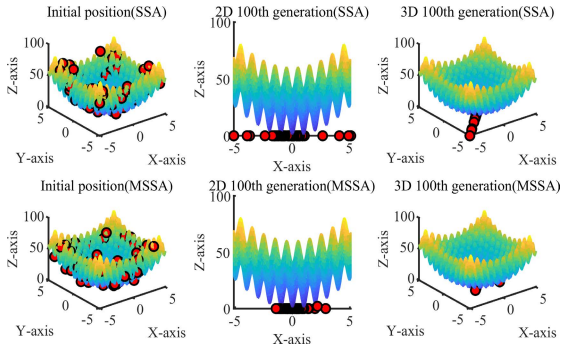

FIGURE 7. Schematic diagram of the motion trajectory of the benchmark function Rastrgin.

seen from Figure 7 that except for a small number of discrete points, most of the population individuals can aggregate to the global optimal value or its vicinity. When looking for the minimum value of the function, some individuals in the standard sparrow search algorithm fall into the local optimum and fail to find the global optimum solution. The results show that compared with SSA, the MSSA algorithm's ability to find the global optimum has been greatly improved. It can be seen from Figure 8 that the optimization of the f_6 is very challenging. Compared with SSA, the MSSA algorithm can see a significant improvement in the optimization trajectory.

In summary, through the processing of various test functions and horizontal and vertical comparison experiments, it is further concluded that MSSA has a strong global search ability and is adaptable to various test functions. Compared with GSO, IASGSO, PSO, APSO, and SSA, the convergence speed and convergence accuracy are significantly improved, which also fully proves the effectiveness and feasibility of the improved algorithm.

V. APPLICATION OF MSSA ALGORITHM IN SERVO SYSTEM

Servo systems have the advantages of fast control response speed and high control accuracy, especially in the case of heavy loads and complex working conditions, as well as good performance, and are widely used in intelligent manufacturing, metallurgy, transportation, aerospace, and other fields. However, a control system based on a hydraulic drive is typically nonlinear. On the one hand, the system parameters are uncertain. However, existing nonlinear control strategies have not achieved satisfactory control effects. Next, we discuss the application example of MSSA in the servo system and the superiority of dealing with the application problems of the actual servo system.

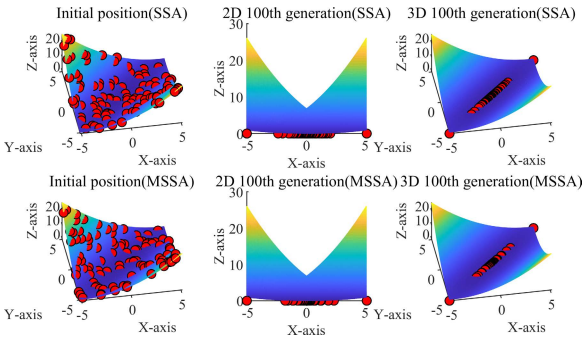

FIGURE 8. Schematic diagram of the motion trajectory of the benchmark function Matyas.

A. PARAMETER IDENTIFICATION PROBLEM OF SERVO SYSTEM

Non-linear friction is one of the main factors that affect the low-speed motion performance of servo systems. Friction causes tracking errors in heavy-duty servo machinery and brings about limited cycle oscillation, slip motion, and other problems [34], [35]. Establishing an accurate friction model is a prerequisite for limiting nonlinear friction, and the mathematical model for parameter identification in the field of lubricating friction is the Stribeck friction model. The steady-state correspondence between the friction torque and rotational speed is:

$$F_f = \left[F_C + (F_S - F_C)\, e^{-\left(\frac{v}{v_s}\right)^2} \right] sgn\,(v) + B_V v \quad (11)$$

where F_f is the friction torque, F_C is the Coulomb friction force, F_S is the static friction force, v_s is the Stribeck velocity, and B_V is the viscous coefficient of friction.

The parameters of the friction model to identify the initial position of the sparrow population are set as:

$$x_{1i}^t = \left[\widehat{F_{Ci}}, \widehat{F_{Si}}, \widehat{v_{si}}, \widehat{B_{Vi}}\right], i = 1, 2, \ldots, N \quad (12)$$

The friction torque identification sequence is:

$$\widehat{F_f} = \left[\widehat{F_C} + \left(\widehat{F_S} - \widehat{F_C}\right) e^{-\left(\frac{v}{\widehat{v_s}}\right)^2} \right] sgn\,(v) + \widehat{B_V} v \quad (13)$$

The identification error is defined as:

$$e_i = F_{fi} - \widehat{F_{fi}}, i = 1, 2, \ldots, N \quad (14)$$

The fitness function adopts the time-multiplied absolute error integration criterion, and its discrete form is designed as follows:

$$f_1 = \sum_{k=0}^{N} k\,|e\,(k)| \quad (15)$$

Furthermore, the problem of friction model parameter identification can be transformed into an optimization problem, and the appropriate friction model parameters are selected through the identification algorithm to make the discrete fitness function between the actual measured friction value and the identified value reach the minimum value.

TABLE 4. Identification values of friction model.

	F_C[0,500]	F_S[0,1000]	v_s[0,1]	B_V[0,100]
PSO	422.0463	609.6192	0.9187569	25.19348
APSO	401.8155	611.7112	0.9888816	29.89739
GSO	415.5599	608.4075	0.9652336	26.59679
IASGSO	416.3335	608.7377	0.9582834	26.4177
SSA	409.7702	607.9196	0.9793255	28.00013
MSSA	411.2345	607.8787	0.9761051	27.62614

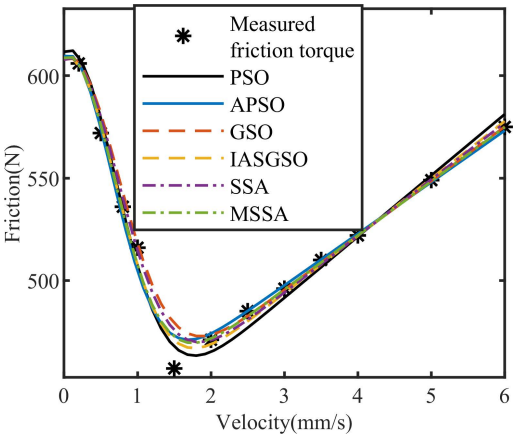

FIGURE 9. Friction torque identification curve.

To verify the performance of the MSSA algorithm, this paper compared the PSO, APSO, GSO, IASGSO, and SSA algorithms, and the parameters were set as follows. For all the algorithms, the population size was set to 50, the maximum number of iterations was set to 500, and the dimension was set to four. Table 4 shows the average value of the optimization results and the optimization range of the six algorithms for the friction model parameter identification problem. Each algorithm was independently run 50 times to obtain the average value.

Considering only the forward phase, the actual collection points of the speed-friction force were 12. Figure 9 shows a schematic of the friction torque and the identification curve measured by the servo system.

It can be seen from Figure 9 that all algorithms that identify the friction torque curve can meet the trend of the measured value of the friction torque. At the speed collection point of 1.5 mm/s, the identification curves cannot be fitted and the error is large. This is constrained by the friction model, and the Stribeck friction model cannot fit the mechanical characteristics of the servo system well. To verify the validity of the parameter identification results, a boxplot was drawn based on the absolute value of the errors of the collection points for each algorithm, as shown in Figure 10. The degree of dispersion reflects the accuracy of identification results.

As shown in Figure 10, the maximum, minimum, median, and upper quartiles in the boxplot of the MSSA algorithm were lower than those of the other algorithms. This shows that the identification friction torque has a better fit with the

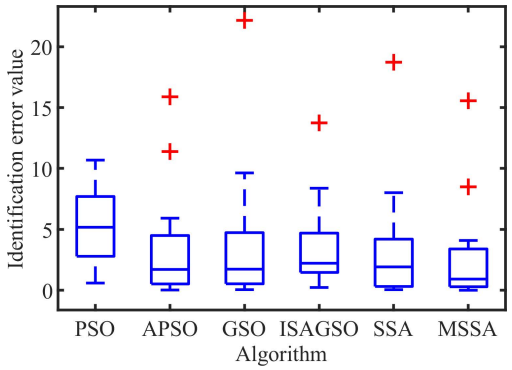

FIGURE 10. Boxplot of identification results.

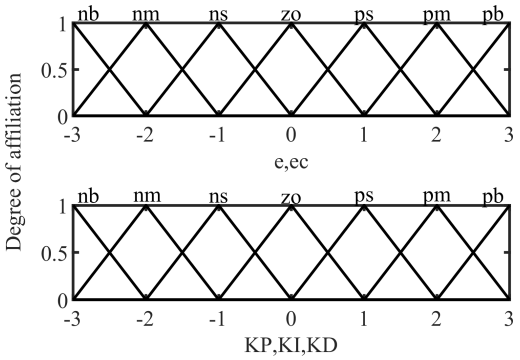

FIGURE 11. Membership function curve diagram.

actual friction torque, the error in the identification value is smaller, and the identification result is more accurate.

In summary, it is shown that MSSA has the best identification results compared to other algorithms, and its application in servo system parameter identification is effective, further demonstrating the superiority of MSSA.

B. CONTROL STRATEGY OPTIMIZATION PROBLEM OF SERVO SYSTEM

1) DESIGN OF MSSA-PID CONTROLLER

The fuzzy PID controller is based on a conventional PID controller. Considering the error of the system's expected output value and feedback value and its rate of change as the input, the online optimization of the proportional, integral, and differential parameters of the PID controller was completed through fuzzy reasoning [36], and a good control effect was obtained. In practical engineering, the values of the scale factor, quantization factor, and initial value of the system parameters significantly affect the dynamic and static performance of the system [37]. The use of manual debugging to select fuzzy parameters has strong limitations, and it is necessary to research new parameter online optimization strategies to improve the control performance of the fuzzy PID controller and further adapt it to the controlled object. Considering the superiority of MSSA, the fuzzy PID self-tuning algorithm based on the fusion multi-strategy evolutionary sparrow search algorithm is designed as follows, which is referred to as the MSSA-fuzzy PID controller.

a: FUZZY QUANTIFICATION OF INPUT AND OUTPUT VARIABLES

The input variables are the error e and the error rate of change e_c, and its quantized universe is [-3,3]. The fuzzy subsets are: {negative large (NB), negative medium (NM), negative small (NS), zero (ZO), positive small (PS), positive medium (PM), positive large (PB)}. The error and the error rate of change are fuzzed by the quantization factors K_e and K_{ec} respectively. The output variables are proportional coefficient K_P, integral coefficient K_I, and differential coefficient K_D, and its quantized universe is [0,3]. The membership function curves of the input and output variables are designed using the symmetrical triangular distribution function, as shown in Figure 11. It is observed that the adjustment amount of the three parameters of the PID controller is:

$$\begin{cases} K_P = k_p + \Delta k_p k_{\Delta p} \\ K_I = k_i + \Delta k_i k_{\Delta i} \\ K_D = k_d + \Delta k_d k_{\Delta d} \end{cases} \tag{16}$$

where Δk_p, Δk_i and Δk_d are the change values after the fuzzy output, $k_{\Delta p}$, $k_{\Delta i}$ and $k_{\Delta d}$ are the fuzzy output scale factors, and k_p, k_i and k_d are the initial values of the systems.

b: THE ESTABLISHMENT OF FUZZY RULES

Fuzzy rules are the core of fuzzy controllers and an important part of the fuzzy inference engine, which determines the effect of fuzzy control. Different errors and error rates of change have different requirements for PID parameters, and the fuzzy rules are shown in Table 5.

c: FUZZY REASONING AND DEFUZZIFICATION

Using MATLAB R2020a as the design tool, the fuzzy PID controller design with a dual-input and three-output structure is completed in the Fuzzy Logic Designer toolbox. The Mamdani fuzzy system modeling method is selected, the area centroid method is used for defuzzification, and the obtained fuzzy output surface is shown in Figure 12.

d: FUZZY PID SELF-TUNING ALGORITHM BASED ON MSSA

To obtain the best control ability, the fuzzy PID parameter tuning problem is transformed into a class of eight-dimensional parameter optimization problems. The eight parameters are regarded as the position of the sparrow, so the optimal solution of the fuzzy PID parameters is regarded as the optimal value of the objective function calculated by the sparrow search algorithm. If the control capability of the fuzzy PID control system satisfies the engineering application or the search range reaches the maximum number of iterations, the optimal solution is selected as the optimal fuzzy PID parameter value.

The chaotic map randomly initializes the position of the sparrow, $x_{2i}^t = \left[\widehat{K_{ei}}, \widehat{K_{eci}}, \widehat{k_{\Delta pi}}, \widehat{k_{\Delta ii}}, \widehat{k_{\Delta di}}, \widehat{k_{pi}}, \widehat{k_{ii}}, \widehat{k_{di}}\right], i = 1, 2, \ldots, N$.

TABLE 5. $K_p/K_i/K_d$ fuzzy rules table.

ec \ e	NB	NM	NS	ZO	PS	PM	PB
NB	PB/NB/ PS	PB/NB/NS	PM/NM/NB	PM/NM/NB	PS/NS/NB	ZO/ZO/NM	ZO/ZO/PS
NM	PB/NB/ PS	PB/NB/NS	PM/NM/NB	PS/NS/NM	PS/NS/NM	ZO/ZO/NS	NS/ZO/ZO
NS	PM/NB/ZO	PM/NM/NS	PM/NS/NM	PS/NS/NM	ZO/ZO/NS	NS/ PS/NS	NS/PS/ZO
ZO	PM/NM/ZO	PM/NM/NS	PS/ NS/NS	ZO/ZO/NS	NS/PS/NS	NM/PM/NS	NM/PM/ZO
PS	PS/NM/ZO	PS/NS/ZO	ZO/ZO/ZO	NS/PS/ZO	NS/PS/ZO	NM/PM/ZO	NM/PB/ZO
PM	PS/ZO/PB	ZO/ZO/NS	NS/ ZO/PS	NM/PS/PS	NM/PM/PS	NM/PB/PS	NB/PB/PB
PB	ZO/ZO/PB	ZO/ZO/PM	NM/NM/PM	NM/NM/PM	NM/PM/PS	NB/NB/PS	NB/ PB/PB

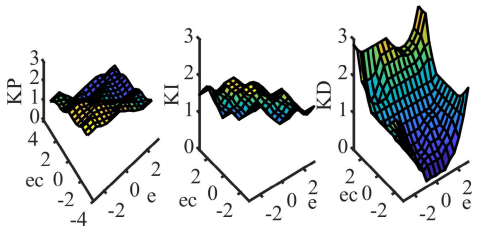

FIGURE 12. Fuzzy control output surface.

To meet the needs of the servo system with small deviation and fast response, and at the same time ensure that the system overshoot is small and the rise time is short. Select the following control performance evaluation functions:

$$f_2 = \int_0^{+\infty} \left(\delta_1 |e(t)| + \delta_2 u^2(t) + \delta_3 |e(t)|\right) dt \qquad (17)$$

where $u(t)$ is the output control quantity, $e(t)$ is the system error, δ is the weight coefficient, $\delta_1 = 1, \delta_2 = 0.002$, $\delta_3 = 120$.

The flowchart of the MSSA-fuzzy PID controller is shown in Figure 13.

2) SIMULATION ENVIRONMENT

The experimental environment adopted Inter(R) Croe(TM) i3-5010UCPU, a PC with a main frequency of 2.1 GHz and a memory of 16 G, the operating system adopts a 32-bit Windows XP system, and the programming language adopts MATLAB R2014b. The model of the electro-hydraulic servo valve in the semi-physical simulation test bench is FF102-30. The rated pressure is 21 MPa, and the rated current is 50 mA. The no-load flow rate is 2.315×10^{-4} m^3/s, the saturation value of the servo amplifier control voltage is ± 10 V, the length of the piston displacement is 35 mm, and the area of the piston rod is 0.001 m^2. The amplification factor of the position sensor is 50 V/m, and the range is 7100 mm. The cylinder stroke is 200 mm and the rated flow is 30 L/min. The oil supply pressure is 4.5 Mpa. Ignoring the viscous damping coefficient, the valve-controlled cylinder model obtained through system identification is shown in Figure 14.

3) SIMULATION AND VERIFICATION

To verify the performance of the MSSA algorithm, we compared the PSO, APSO, GSO, IASGSO, and SSA algorithms

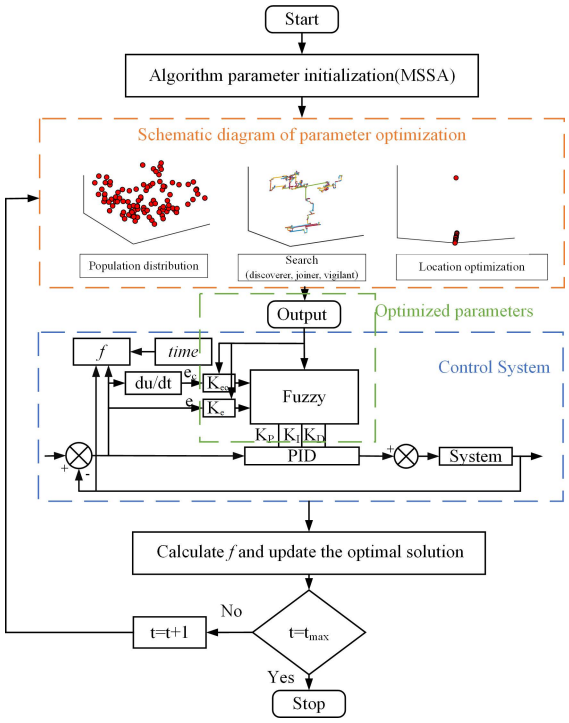

FIGURE 13. Schematic diagram of control strategy.

using the parameters. For all algorithms, the population size is set to 50, the maximum number of iterations is set to 100, and the dimension is set to eight. The search space for the initial value of the fuzzy PID parameters is [0,50], and the search space for the quantization and scale factors is [0,1]. Twenty independent runs were performed for each optimization method, and their averages were recorded.

C. STEP RESPONSE

The input signal adopts a step signal with a position amplitude of 20 mm, simulation time of 2s, and sampling time of 0.001s. The input and output response curves and locally enlarged diagrams are shown in Figure 15, and the performance indicators of the control system optimization results are listed in Table 6.

The transient response reflects the reliability and regulation accuracy of a control system. Steady-state value ym (mm), overshoot σ (%), delay time tr (s), peak time tm (s),

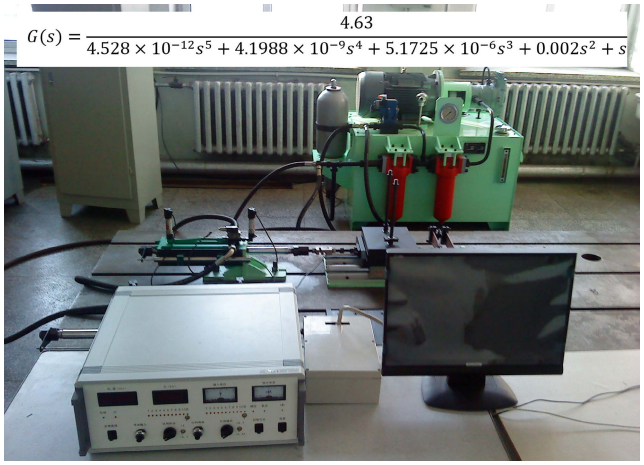

FIGURE 14. Semi-physical servo system simulation test bench.

TABLE 6. Performance indicators of control system optimization results.

	PSO	APSO	GSO	IASGSO	SSA	MSSA
f	1.7E-2	4.3E-3	2.8E-2	4.0E-3	3.4E-3	7.8E-4
y_m	20.05	20.02	20.08	20.04	20.05	20.00
t_r	0.537	0.539	0.555	0.535	0.527	0.526
t_m	0.6107	0.624	0.6527	0.613	0.581	0.580
t_s	0.554	0.565	0.592	0.558	0.545	0.544
σ	2.544	0	0	0	0	0

adjustment time ts (s), and other indicators. σ represents the difference between the maximum output signal and the ideal output signal. tr represents the running time from the output signal to the semi-steady state. tm is the run time required to maximize the working signal. ts is the run time required to maintain the output signal within a steady-state error of $\pm 2\%$.

The response curve of the control system optimized by MSSA converges to the optimal steady-state value, whereas the system has an overshoot after optimization by PSO, and the SSA exhibits some slight oscillations. Compared with other algorithms, MSSA is better in terms of the rising time, peak value, and settling time. The response curve has the advantages of small overshoot, short rise time, and adjustment time, which make the system less prone to oscillation and can quickly reach a stable state. This also demonstrates the superiority and feasibility of the algorithm improvement.

D. SINUSOIDAL RESPONSE

The input signal is a sinusoidal signal with a position amplitude of 20 mm, the angular frequency is set to 1.6π and 3.2π (rad/s), the simulation time is set to 2 s, and the sampling time is set to 0.001 s. Figure 16 shows the input-output response curve and position error curve, and Table 7 shows the maximum position error.

Combining Table 7 and Figure 16, the difference between the output amplitude of the control system through the GSO algorithm and the ideal amplitude is the largest. The MSSA is closest to the ideal amplitude, which effectively improves the tracking accuracy compared with other control methods.

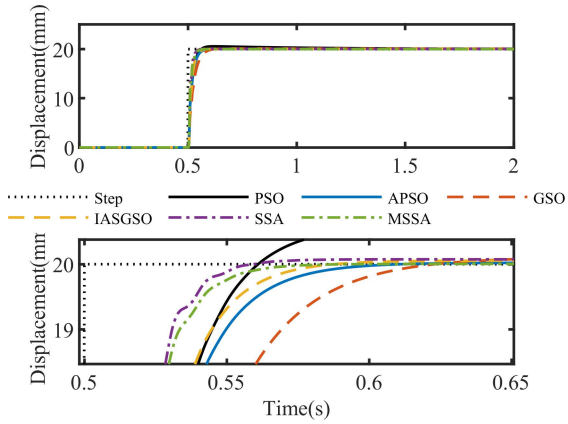

FIGURE 15. Step signal input and output response curve.

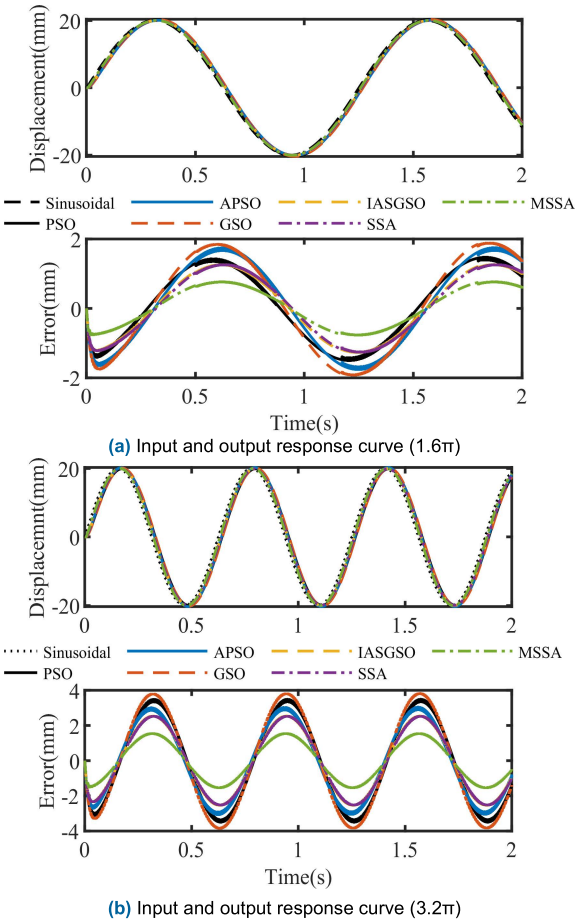

FIGURE 16. Sinusoidal signal input and output response curve.

In particular, when the input signal adopts a 1.6π sinusoidal signal, the maximum position error of MSSA is 37.98% higher than that of SSA, 38.46% higher than that of IASGSO, 57.45% higher than that of GSO, 54.29% higher than that of APSO, and 44.06% higher than that of PSO. It is demonstrated that the proposed controller has good robustness.

E. TRIANGLE WAVE RESPONSE

The input signal is a triangular wave signal, the position amplitude is 20 mm, the period is set to 1 and 0.5 s, the

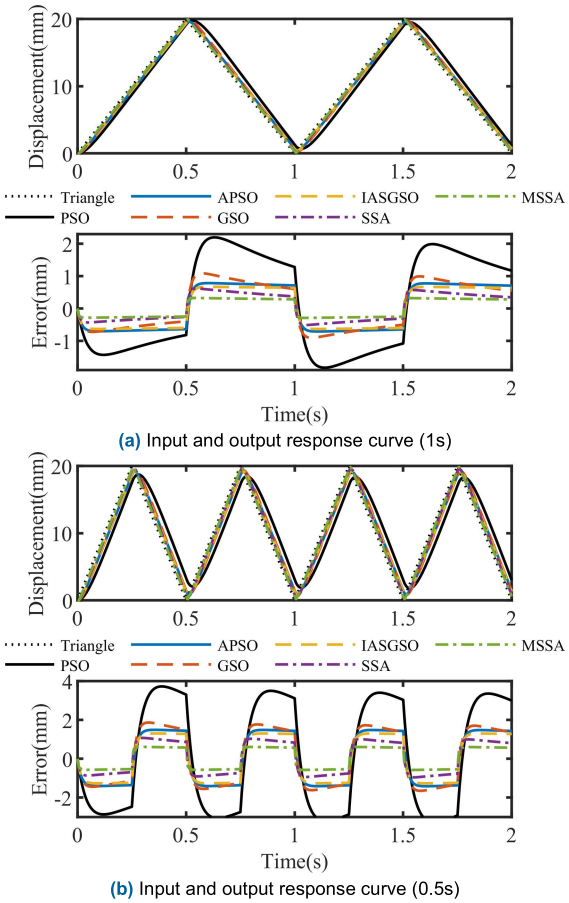

(a) Input and output response curve (1s)

(b) Input and output response curve (0.5s)

FIGURE 17. Triangular wave signal input and output response curve.

TABLE 7. Maximum position error of sinusoidal input signal.

	PSO	APSO	GSO	IASGSO	SSA	MSSA
1.6 π	1.43	1.75	1.88	1.30	1.29	0.80
3.2 π	3.46	3.00	3.85	2.58	2.57	1.60

simulation time is set to 2 s, and the sampling time is 0.001 s. Its input-output response curve and position error curve are shown in Figure 17, and Table 8 shows the maximum position error.

Combining Table 8 and Figure 17, with a reduction in the period, the control error increases, and the position error of the PSO algorithm is the largest. In particular, the input signal adopts a triangular wave signal with a period of 1 s, the maximum position error of MSSA is 48.39% higher than that of SSA, 52.24% higher than that of IASGSO, 70.64% higher than that of GSO, 58.97% higher than that of APSO, and 85.45% higher than that of PSO. Compared with other algorithms, MSSA shows better control performance in terms of steady-state accuracy and dynamic response.

F. PERTURBATION SIGNAL

The input signal selects a sinusoidal signal and adds Gaussian white noise perturbation and a sudden perturbation. The amplitude of the sinusoidal signal position is 20mm, the

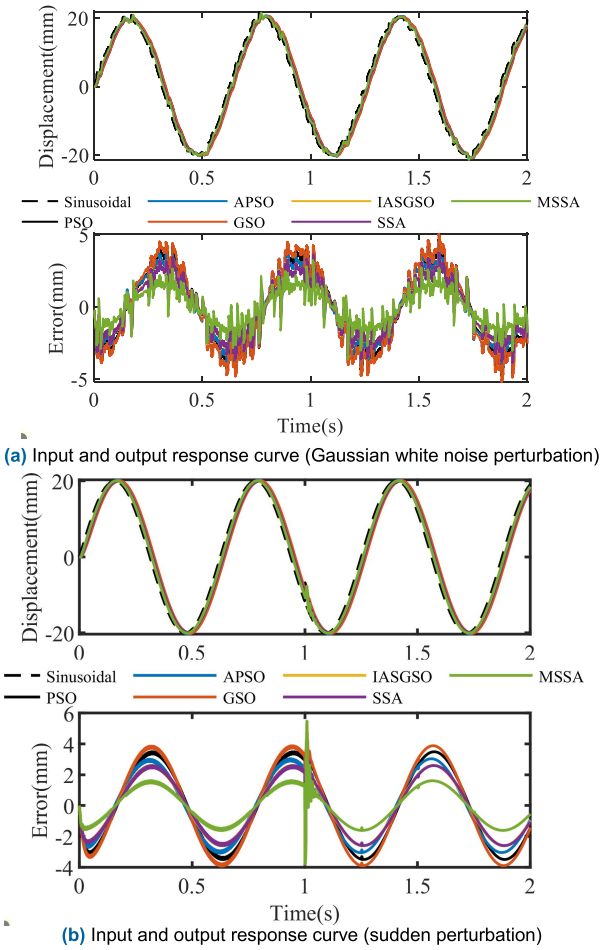

(a) Input and output response curve (Gaussian white noise perturbation)

(b) Input and output response curve (sudden perturbation)

FIGURE 18. Disturbance signal input and output response curve.

angular frequency is set to 1.6π (rad/s), the simulation time is set to 2 s, and the sampling time is set to 0.001s. Figure 18 shows the input and output response and position error curves, and Table 9 shows the maximum position error.

Combining Table 9 and Figure 18, after adding the Gaussian white noise perturbation, each output curve fluctuates to different degrees. Among them, MSSA has the smallest error change and can quickly suppress the perturbation signal compared with other control methods. In particular, the input signal is sinusoidal with Gaussian white noise added, the maximum position error of MSSA is 17.87% higher than that of SSA, 18.13% higher than that of IASGSO, 41.90% higher than that of GSO, 28.61% higher than that of APSO, and 36.25% higher than that of PSO. After adding the sudden disturbance, the error change of the MSSA is the largest, but it is observed that the recovery speed of the MSSA is the fastest. Overall, the results show that the MSSA can quickly respond to sudden disturbance.

The above simulation experiments show that the MSSA online optimization of fuzzy PID parameters improves the dynamic and static performance and robustness of the system. The feasibility and effectiveness of MSSA in optimizing fuzzy PID parameters are further illustrated, and it is found

TABLE 8. Maximum position error of triangular wave input signal.

	PSO	APSO	GSO	IASGSO	SSA	MSSA
1 s	2.20	0.78	1.09	0.67	0.62	0.32
0.5 s	3.73	1.49	1.86	1.30	1.07	0.61

TABLE 9. Maximum position error of disturbance input signal.

	PSO	APSO	GSO	IASGSO	SSA	MSSA
Gaussian white	4.11	3.67	4.51	3.20	3.19	2.62
Sudden	4.80	4.48	4.81	4.68	4.73	5.47

to be superior to conventional methods. This control strategy has a good control effect when dealing with a nonlinear servo system.

In summary, by comparing the results of the practical application examples of the above two servo systems, it can be found that the MSSA proposed in this research has certain advantages in the optimization of practical engineering design problems, which further reflects the robustness of MSSA. The designed MSSA-fuzzy PID control strategy can achieve good results, verifying the effectiveness of the proposed control strategy.

VI. CONCLUSION

To improve the insufficient distribution of the population in the initialization stage of the sparrow search algorithm (SSA), which is easily disturbed by the local optimal solution during the optimization process, a multi-strategy improved evolutionary sparrow search algorithm (MSSA) is proposed. The three key improvements to MSSA are as follows.

1. By analyzing the initial distribution of the population, the tent chaotic sequence is introduced to improve the initial population diversity of the algorithm.

2. Give a sparrow finder random search ability to improve the searchability of the algorithm.

3. Perform mutation evolution operations on sparrow individuals that are found to be dangerous, and combine greedy strategies to prevent the algorithm from falling into local optimal solutions.

To prove the superiority of the proposed algorithm, six test functions are used to verify the superiority of the algorithm from four aspects: optimization ability, robustness, convergence ability, and optimization trajectory. Simulation results demonstrate the effectiveness and superiority of the proposed algorithm.

Combined with two servo system application examples, the parameter identification of the servo system friction model shows that the MSSA algorithm has better optimization and identification capabilities. A servo system control strategy is designed that organically combines MSSA and fuzzy PID. The tracking performance and stability of the proposed control strategy are demonstrated using different input signals. Simulation experiments demonstrate that the control strategy improves the control performance of the servo system. In particular, the input signal adopts a triangular wave signal with a period of 1s, the maximum position error of MSSA is 48.39% higher than that of SSA, 52.24% higher than that of IASGSO, 70.64% higher than that of GSO, 58.97% higher than that of APSO, and 85.45% higher than that of PSO. The effectiveness of the MSSA in practical engineering applications and the feasibility of the proposed control strategy are further verified.

MSSA is a meta-heuristic algorithm that has been proposed recently, and there are still many areas to discuss and improve. This research is only an improvement in the research attempt. In future work, it can be considered to introduce other intelligent algorithms in SSA, explore new optimization schemes, improve the robustness and adaptability of SSA, and expand its application field.

ACKNOWLEDGMENT

The authors would like to thank the anonymous reviewers and Academic Editor for their valuable and constructive comments, which greatly improved the quality and integrity of this manuscript.

REFERENCES

[1] M. Mavrovouniotis, F. M. Müller, and S. Yang, "Ant colony optimization with local search for dynamic traveling salesman problems," *IEEE Trans.*, vol. 47, no. 7, pp. 1743–1756, Jul. 2017.

[2] S. Ding, W. Du, X. Zhao, L. Wang, and W. Jia, "A new asynchronous reinforcement learning algorithm based on improved parallel PSO," *Int. J. Speech Technol.*, vol. 49, no. 12, pp. 4211–4222, May 2019.

[3] E. Bernal, M. L. Lagunes, O. Castillo, J. Soria, and F. Valdez, "Optimization of type-2 fuzzy logic controller design using the GSO and FA algorithms," *Int. J. Fuzzy Syst.*, vol. 23, no. 1, pp. 42–57, Feb. 2021.

[4] M. A. Memon, M. D. Siddique, S. Mekhilef, and M. Mubin, "Asynchronous particle swarm optimization-genetic algorithm (APSO-GA) based selective harmonic elimination in a cascaded H-bridge multilevel inverter," *IEEE Trans. Ind. Electron.*, vol. 69, no. 2, pp. 1477–1487, Feb. 2022.

[5] S. Nasrollahzadeh, M. Maadani, and M. A. Pourmina, "Optimal motion sensor placement in smart Homes and intelligent environments using a hybrid WOA-PSO algorithm," *J. Reliable Intell. Environ.*, Sep. 2021.

[6] T. S. L. V. Ayyarao, N. S. S. Ramakrishna, R. M. Elavarasan, N. Polumahanthi, M. Rambabu, G. Saini, B. Khan, and B. Alatas, "War strategy optimization algorithm: A new effective Metaheuristic algorithm for global optimization," *IEEE Access*, vol. 10, pp. 25073–25105, 2022.

[7] B. Alatas, "ACROA: Artificial chemical reaction optimization algorithm for global optimization," *Expert Syst. Appl.*, vol. 38, no. 10, pp. 13170–13180, May 2011.

[8] J. Xue and B. Shen, "A novel swarm intelligence optimization approach: Sparrow search algorithm," *Syst. Sci. Control Eng.*, vol. 8, no. 1, pp. 22–34, Jan. 2020.

[9] N. A. A. Aziz, Z. Ibrahim, M. Mubin, and S. Sudin, "Adaptive switching gravitational search algorithm: An attempt to improve diversity of gravitational search algorithm through its iteration strategy," *Sādhanā*, vol. 42, no. 7, pp. 1103–1121, Jun. 2017.

[10] B. Alatas and H. Bingol, "A physics based novel approach for travelling tournament problem: Optics inspired optimization," *Inf. Technol. Control*, vol. 48, no. 3, pp. 373–388, Sep. 2019.

[11] Z. C. Deng, H. Sun, and J. Zhao, "Particle swarm optimization with square wave triggered exploration and exploitation," *Acta Automatica Sinica*, to be published, doi: 10.16383/j.aas.c190842.

[12] J. Liu, H. Peng, Z. Wu, J. Chen, and C. Deng, "Multi-strategy brain storm optimization algorithm with dynamic parameters adjustment," *Int. J. Speech Technol.*, vol. 50, no. 4, pp. 1289–1315, Apr. 2020.

[13] T. Zhang, Q. Zeng, and X. Zhao, "Optimal local dimming based on an improved greedy algorithm," *Int. J. Speech Technol.*, vol. 50, no. 12, pp. 4162–4175, Dec. 2020.
[14] X.-W. Yu, L.-P. Huang, Y. Liu, K. Zhang, P. Li, and Y. Li, "WSN node location based on beetle antennae search to improve the gray wolf algorithm," *Wireless Netw.*, vol. 28, no. 2, pp. 539–549, Jan. 2022.
[15] B. Alatas and H. Bingol, "Comparative assessment of light-based intelligent search and optimization algorithms," *Light Eng.*, vol. 28, no. 6, pp. 51–59, 2020.
[16] T. Wang, X.-W. Fu, and X.-G. Gao, "Cooperative task assignment for heterogeneous multi-UAVs based on improved genetic algorithm," *Fire Control Command Control*, vol. 38, no. 5, pp. 37–41, May 2013.
[17] T. Liu, Z. Yuan, L. Wu, and B. Badami, "Optimal brain tumor diagnosis based on deep learning and balanced sparrow search algorithm," *Int. J. Imag. Syst. Technol.*, vol. 31, no. 4, pp. 1921–1935, Dec. 2021.
[18] S. Akyol and B. Alatas, "Plant intelligence based metaheuristic optimization algorithms," *Artif. Intell. Rev.*, vol. 47, no. 4, pp. 417–462, May 2017.
[19] H. Mohammed and T. Rashid, "A novel hybrid GWO with WOA for global numerical optimization and solving pressure vessel design," *Neural Comput. Appl.*, vol. 32, no. 18, pp. 14701–14718, Mar. 2020.
[20] Y. Yu, Y. Xu, F. Wang, W. Li, X. Mai, and H. Wu, "Adsorption control of a pipeline robot based on improved PSO algorithm," *Complex Intell. Syst.*, vol. 7, no. 4, pp. 1797–1803, Aug. 2021.
[21] L. X. Wei, Y. K. Zhang, and H. Sun, "Robot dynamic path planning based on improved ant colony and DWA algorithm," *Control Decision*, to be published, doi: 10.13195/j.kzyjc.2021.1804.
[22] H. Bingol and B. Alatas, "Chaos based optics inspired optimization algorithms as global solution search approach," *Chaos, Solitons Fractals*, vol. 141, Dec. 2020, Art. no. 110434.
[23] Z. Zhang, R. He, and K. Yang, "A bioinspired path planning approach for mobile robots based on improved sparrow search algorithm," *Adv. Manuf.*, vol. 10, no. 1, pp. 114–130, Mar. 2022.
[24] A. Tang, H. Zhou, T. Han, and L. Xie, "A chaos sparrow search algorithm with logarithmic spiral and adaptive step for engineering problems," *Comput. Model. Eng. Sci.*, vol. 130, no. 1, pp. 331–364, 2021.
[25] B. Alatas, "Chaotic bee colony algorithms for global numerical optimization," *Expert Syst. Appl.*, vol. 37, no. 8, pp. 5682–5687, Feb. 2010.
[26] E. V. Altay and B. Alatas, "Bird swarm algorithms with chaotic mapping," *Artif. Intell. Rev.*, vol. 53, no. 2, pp. 1373–1414, Apr. 2020.
[27] H. Bingol and B. Alatas, "Chaotic league championship algorithms," *Arabian J. Sci. Eng.*, vol. 41, no. 12, pp. 5123–5147, May 2016.
[28] X. Li, J. Gu, X. Sun, J. Li, and S. Tang, "Parameter identification of robot manipulators with unknown payloads using an improved chaotic sparrow search algorithm," *Appl. Intell.*, pp. 1–11, Jan. 2022.
[29] B. Alatas, "Chaotic harmony search algorithms," *Appl. Math. Comput.*, vol. 216, no. 3, pp. 2687–2699, Mar. 2010.
[30] J. Dong, Z. Dou, S. Si, Z. Wang, and L. Liu, "Optimization of capacity configuration of wind–solar–diesel–storage using improved sparrow search algorithm," *J. Electr. Eng. Technol.*, vol. 17, no. 1, pp. 1–14, Jul. 2022.
[31] B. Lei and J.-L. Fan, "Adaptive kaniadakis entropy thresholding segmentation algorithm based on particle swarm optimization," *Soft Comput.*, vol. 24, no. 10, pp. 7305–7318, Sep. 2020.
[32] M. Lu, H. Wang, J. Lin, A. Yi, Y. Gu, and D. Zhao, "A nonlinear Wiener system identification based on improved adaptive step-size glowworm swarm optimization algorithm for three-dimensional elliptical vibration cutting," *Int. J. Adv. Manuf. Technol.*, vol. 103, nos. 5–8, pp. 2865–2877, Apr. 2019.
[33] Y. Fan, J. Shao, G. Sun, and X. Shao, "Proportional–integral–derivative controller design using an advanced Lévy-flight salp swarm algorithm for hydraulic systems," *Energies*, vol. 13, no. 2, p. 459, Jan. 2020.
[34] C.-Y. Lee, S.-H. Hwang, E. Nam, and B.-K. Min, "Identification of mass and sliding friction parameters of machine tool feed drive using recursive least squares method," *Int. J. Adv. Manuf. Technol.*, vol. 109, nos. 9–12, pp. 2831–2844, Aug. 2020.
[35] M. Liang and D. Zhou, "A nonlinear friction identification method combining separable least squares approach and kinematic orthogonal property," *Int. J. Precis. Eng. Manuf.*, vol. 23, no. 2, pp. 139–152, Jan. 2022.
[36] N. D. Phu, N. N. Hung, A. Ahmadian, and N. Senu, "A new fuzzy PID control system based on fuzzy PID controller and fuzzy control process," *Int. J. Fuzzy Syst.*, vol. 22, no. 7, pp. 2163–2187, Aug. 2020.
[37] X. Wang, "Development and simulation of fuzzy adaptive PID control for time variant and invariant systems," *Int. J. Syst. Assurance Eng. Manage.*, pp. 1–9, Aug. 2021.

BINGWEI GAO received the B.S. and Ph.D. degrees from the Harbin University of Science and Technology, Harbin, Heilongjiang, China, in 2010 and 2015, respectively.

She is currently a Lecturer with the Harbin University of Science and Technology. She has published over 30 papers in domestic and international academic journals and conference proceedings. Her main research interests include electro-hydraulic servo control and hydraulic quadruped robot.

WEI SHEN received the B.S. degree in mechanical design and automation from the Xuzhou University of Technology, Xuzhou, Jiangsu, China, in 2020. He is currently pursuing the M.S. degree with the Harbin University of Science and Technology, Harbin, Heilongjiang, China.

His research interests include swarm intelligence optimization algorithms and electro-hydraulic servo control.

HAO GUAN received the B.S. degree in mechanical design manufacture and automation major from the Heilongjiang University of Technology, Jixi, Heilongjiang, China, in 2019. He is currently pursuing the M.S. degree with the Harbin University of Science and Technology, Harbin, Heilongjiang.

His research interest includes hydraulic servo control.

LINTAO ZHENG received the B.S. degree in mechanical design, manufacturing, and automation from the Wuhan Institute of Bioengineering, Wuhan, Hubei, China, in 2021. He is currently pursuing the M.S. degree with the Harbin University of Science and Technology, Harbin, Heilongjiang, China.

His research interest includes hydraulic servo control.

WEI ZHANG received the B.S. degree in vehicle engineering from Shenyang Aerospace University, Shenyang, Liaoning, China, in 2021. He is currently pursuing the M.S. degree with the College of Mechanical and Power Engineering, Harbin University of Science and Technology, Harbin, China.

His research interest includes electro-hydraulic servo control.